Published OnlineFirst February 3, 2015; DOI: 10.1158/0008-5472.CAN-14-1589

Tumor and Stem Cell Biology

Cancer Research

CYP3A5 Functions as a Tumor Suppressor in Hepatocellular Carcinoma by Regulating mTORC2/Akt Signaling

Feng Jiang[1,2,3], Lei Chen[1,4], Ying-Cheng Yang[1], Xian-ming Wang[1], Ruo-Yu Wang[1], Liang Li[1], Wen Wen[1], Yan-Xin Chang[1], Cai-Yang Chen[1], Jing Tang[1], Gao-Mi-Yang Liu[1], Wen-Tao Huang[1], Lin Xu[2,3], and Hong-Yang Wang[1,4]

Abstract

CYP3A5 is a cytochrome P450 protein that functions in the liver metabolism of many carcinogens and cancer drugs. However, it has not been thought to directly affect cancer progression. In this study, we challenge this perspective by demonstrating that CYP3A5 is downregulated in many hepatocellular carcinomas (HCC), where it has an important role as a tumor suppressor that antagonizes the malignant phenotype. CYP3A5 was downregulated in multiple cohorts of human HCC examined. Lower CYP3A5 levels were associated with more aggressive vascular invasion, poor differentiation, shorter time to disease recurrence after treatment, and worse overall patient survival. Mechanistic investigations showed that CYP3A5 overexpression limited MMP2/9 function and suppressed HCC migration and invasion *in vitro* and *in vivo* by inhibiting AKT signaling. Notably, AKT phosphorylation at Ser473 was inhibited in CYP3A5-overexpressing HCC cells, an event requiring mTORC2 but not Rictor/mTOR complex formation. CYP3A5-induced ROS accumulation was found to be a critical upstream regulator of mTORC2 activity, consistent with evidence of reduced GSH redox activity in most clinical HCC specimens with reduced metastatic capacity. Taken together, our results defined CYP3A5 as a suppressor of HCC pathogenesis and metastasis with potential utility a prognostic biomarker. *Cancer Res; 75(7); 1470–81. ©2015 AACR.*

Introduction

The cytochrome P450s (P450) are involved in the response to cancer treatment and the initiation and promotion of tumorigenesis (1, 2). CYP3A are the main members of P450s that contribute to drug metabolism and metabolize a variety of endogenous substrates. CYP3A4 is the most abundant of CYP3A isoforms in human livers and the major enzyme involved in xenobiotic metabolism that can activate several procarcinogens and also has critical roles in the metabolism of various anticancer drugs upon chemotherapy (3, 4). Moreover, CYP3A4 is reported to have a positive correlation with malignant hepatocellular carcinoma (HCC) characteristics and facilitates proliferation of cancer cells *in vitro* (5–7). In comparison, CYP3A5, the best investigated of the minor CYP3A isoforms, is also involved in the metabolism of drugs, exogenous carcinogens, and endogenous molecules (8). The human *CYP3A5* gene is located on chromosome 7q21.1 and spans approximately 32 kb in length within the CYP3A gene cluster (9). Recently, most studies about CYP3A5 have addressed the relationship of CYP3A5 SNP (or genotype) polymorphism and cancer risk or drug metabolism (8, 10). So far, at least 34 SNPs of the *CYP3A5* gene have been identified (11). Among them, the most frequent and functional polymorphism is the A to G transition in intron 3 at position 6986 (CYP3A5*3, rs776746 A>G), which is associated with CYP3A5 protein production and enzyme activity (11). Until now, the potential role of CYP3A5 in HCC metastasis and invasion remains largely unknown.

In the current study, we focused on the physiologic functions of CYP3A5 on tumor progression rather than its epidemiologic-related consequences. Contrary to CYP3A4 (5, 7), the aberrantly decreased expression of CYP3A5 in HCC and a negative association between CYP3A5 expression and malignant HCC characteristics were observed in a large HCC cohort. More, exogenous expression of CYP3A5 dramatically suppressed HCC migration and invasion through inhibiting ROS/mTORC2/p-AKT (S473) signaling.

Materials and Methods

Immunohistochemistry and tissue microarray analysis

This study was approved by the Eastern Hepatobiliary Surgery Hospital Research Ethics Committee. The detailed information of each patient was obtained from hospital charts and referring

[1]International Co-operation Laboratory on Signal Transduction, Eastern Hepatobiliary Surgery Institute, Second Military Medical University, Shanghai, China. [2]Department of Thoracic Surgery, Cancer Hospital of Jiangsu Province, Cancer Institution of Jiangsu Province, Affiliated Cancer Hospital of Nanjing Medical University, Nanjing, China. [3]Jiangsu Key Laboratory of Molecular and Translational Cancer Research, Cancer Hospital of Jiangsu Province, Nanjing, China. [4]National Center for Liver Cancer, Shanghai, China.

Note: Supplementary data for this article are available at Cancer Research Online (http://cancerres.aacrjournals.org/).

F. Jiang, L. Chen, and Y.-C. Yang contributed equally to this article.

Corresponding Authors: Hong-Yang Wang, Eastern Hepatobiliary Surgery Institute, Second Military Medical University, No. 225, Changhai Road, Shanghai 200438, China. Phone: 8621-8187-5361; Fax: 8621-6556-6851; E-mail: hywangk@vip.sina.com; and Lin Xu, No.42, Baiziting Road, Jiangsu, China. Phone: 86-25-83284701; E-mail: xulin_83@hotmail.com

doi: 10.1158/0008-5472.CAN-14-1589

Published OnlineFirst February 3, 2015; DOI: 10.1158/0008-5472.CAN-14-1589

physicians. Immunohistochemistry of HCC tissue microarray slides was performed using the respective antibodies. Briefly, the slides were probed with primary antibodies specific for the CYP3A5 protein. Anti-rabbit horseradish peroxidase-conjugated secondary antibodies (Santa Cruz Biotechnology) were applied. Finally, diaminobenzidine (DAB) colorimetric reagent solution from Dako was used and followed by hematoxylin counterstaining (Sigma). Reading of the HCC tissue microarray was performed by scanning the slides with an Aperio ScanScope GL, and the Aperio ImageScope software (Aperio Technologies) was used to assess the scanned images based on the percentage of positively stained cells and the staining intensity. Expression levels of CYP3A5 in all tissue samples were quantified, and the CYP3A5 expression level between each pair tumor/peri-tumor was compared.

In vitro cell behavior assays

For the migration and invasion assays, Transwell filter chambers (Costar) and BioCoat Matrigel invasion chambers (BD Biosciences) were used according to the manufacturer's instructions. Six random microscopic fields were counted per field for each group, and these experiments were repeated at least three times independently. Cell adhesion assays were performed using the CytoSelect 48-Well Cell Adhesion Assay Kit (fibronectin-coated) according to the manufacturer's instructions (CellBiolabs). For the cell proliferation assays, SMMC-7721-CYP3A5, HCC-LM3-CYP3A5 and control cells (1×10^3/well) were seeded in 100 μL of growth medium in 96-well plates for various time periods. Cell proliferation was evaluated by measuring cell viability with the CCK-8 assay (Dojindo Laboratories) according to the manufacturer's instructions.

Zymograph assay

Protein was collected from SMMC-7721 and HCC-LM3 cells and processed. Total protein for each sample (15 μg) was electrophoresed on 10% SDS-PAGE gel containing 0.1% gelatin under nonreducing conditions. Gelatin zymography was performed using a MMP Zymography Assay Kit (Applygen Technologies Inc.) according to the manufacturer's protocol. Gelatinolytic bands were observed as clear zones against the blue background and the image intensity was estimated using the Scnlmage Software.

The conduction of multivariate correlation

Kaplan–Meier analysis was used to assess survival. Log-rank tests were used to compare patient survival between subgroups. Multivariate analyses were performed using the Cox multivariate proportional hazard regression model in a stepwise manner (forward, likelihood ratio). The data are presented as the mean ± SD unless otherwise indicated. Differences were considered to be statistically significant for P values < 0.05. For the CYP3A5 staining density analyses, the cut-off value for defining the subgroups was the median. The samples were then divided into two groups. One group was composed of samples in which the CYP3A5 expression levels were above the median value, and the other group was composed of the remaining samples. Each data set was analyzed separately.

Total phosphatidic acid assay

The total phosphatidic acid in each cell line was measured using the Total Phosphatidic Acid Assay Kit (KA1383; Abnova) according to the manufacturer's instructions. The final phosphatidic acid level in each cell line was calculated to standardize the phosphatidic acid concentration in each sample to protein concentration.

ROS detection and GSH measurement

Production of reactive oxygen species (ROS) was measured with the CellROX Deep Red Reagent Kit (Life Technologies Corporation). Briefly, cells were preincubated with the CellROX Reagent at a final concentration of 5 μmol/L for 30 minutes at 37°C. After the extracellular dye was removed, the cells were washed 3 times, and incubated with serum-free DMEM. Nuclei were counterstained with DAPI before imaging. The production of intracellular ROS was detected via confocal laser scanning microscopy (Leica). Total liver glutathione (GSH) content were determined by a commercial kit (Jiancheng) according to the manufacturer's protocol. GSH and GSSG Levels were measured using a GSH and GSSG Assay Kit (Beyotime).

mTORC2 immunoprecipitations and *in vitro* kinase assay

For immunoprecipitation experiments, the lysis buffer contained 0.3% CHAPS instead of 1% Triton to preserve the integrity of the mTOR complexes. Two micrograms of Rictor antibody was added to the cleared cellular lysates (1 mg of protein content in 700 μL) and incubated with rotation at 4°C for 90 minutes. After 1 hour of incubation with 40 μL of 50% slurry of protein A/G–agarose, immunoprecipitates captured by protein A/G–agarose were washed four times with CHAPS-containing lysis buffer and once with the mTORC2 kinase reaction buffer [25 mmol/L Hepes (pH 7.5), 100 mmol/L potassium acetate, and 2 mmol/L $MgCl_2$]. For *in vitro* mTORC2 kinase reactions, immunoprecipitates were incubated in a final volume of 15 μL at 37°C for 20 minutes in the kinase buffer containing 500 ng of inactive AKT1 and 500 mmol/L ATP. The reaction was stopped by the addition of 200 μL of ice-cold enzyme dilution buffer [20 mmol/L Mops (pH 7.0), 1 mmol/L EDTA, 0.3% CHAPS, 5% glycerol, 0.1% 2-mercaptoethanol, and bovine serum albumin (BSA; 1 mg/mL)]. After a quick spin, the supernatant was removed from the protein A/G–agarose, and a 15 μL portion was analyzed by immunoblotting for p-AKT (S473) and total AKT. The pelleted protein A/G–agarose beads were also analyzed by immunoblotting to determine the abundance of Rictor and mTOR in the immunoprecipitates.

Statistical analysis

All results were expressed as mean ± SD. Differences between the experimental and control groups were assessed by either the ANOVA or nonparametric tests, as applicable, using SPSS 17.0 (SPSS, Inc.). Survival analyses were plotted using the Kaplan–Meier method, and the differences between groups were analyzed using the log-rank test. $P < 0.05$ was considered statistically significant.

Results

CYP3A5 is frequently downregulated in HCC tissues and is negatively associated with metastatic potential

To identify the potential difference of CYP3A5 expression between HCC and adjacent normal tissues, the data from TCGA (The Cancer Genome Atlas) and GEO (Gene Expression Omnibus, GSE36763, GSE14520, GSE22058) were statistically analyzed, in which frequently downregulated expression of CYP3A5 was observed in tumor tissues in comparison with

Published OnlineFirst February 3, 2015; DOI: 10.1158/0008-5472.CAN-14-1589

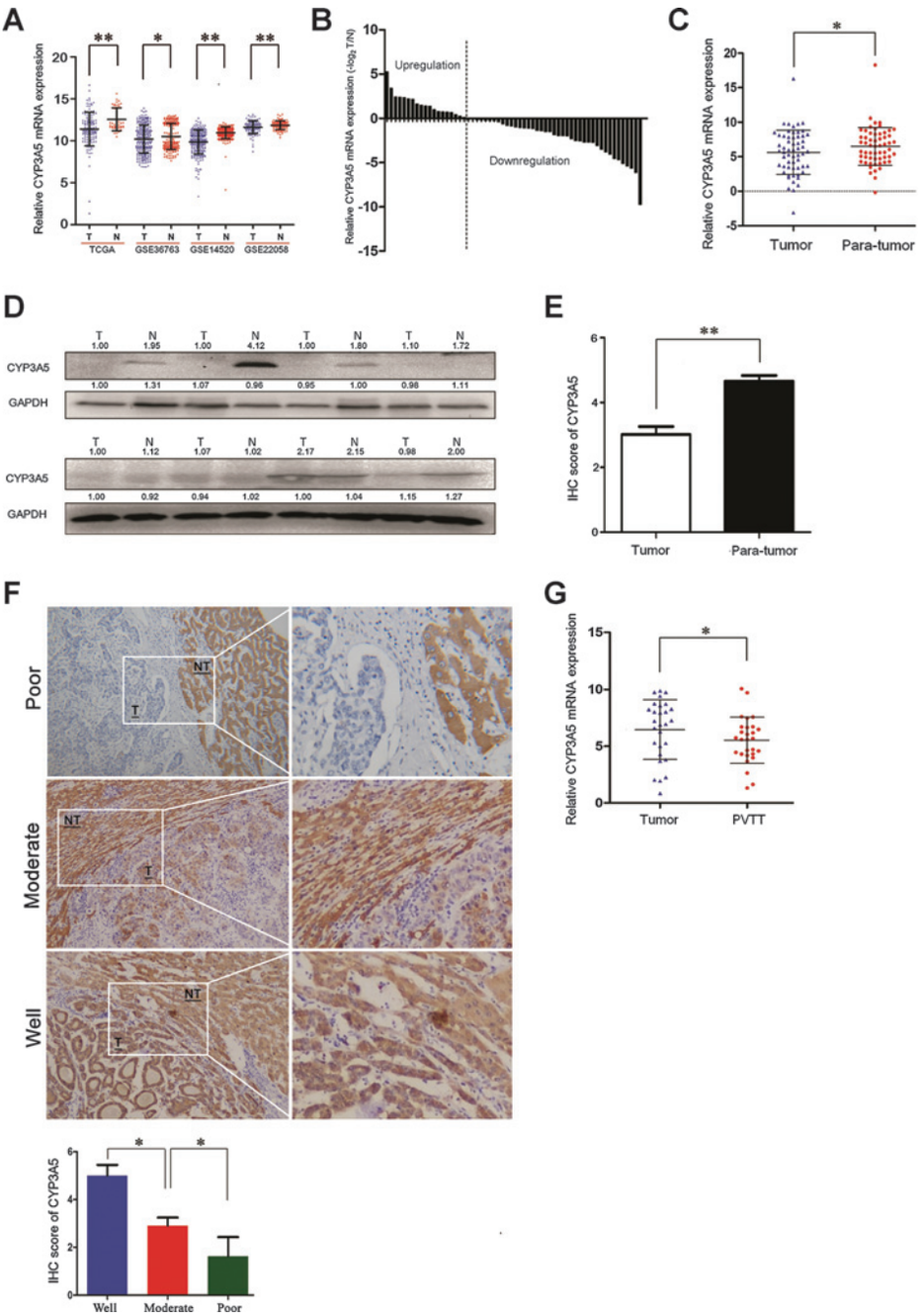

Figure 1.
CYP3A5 level is downregulated in HCC tissues and is negatively associated with metastatic potential. A, the gene chip data of HCC were obtained from TCGA and GEO databases, and the expression levels of CYP3A5 mRNA in HCC and adjacent nontumor tissues were statistically analyzed (*, $P < 0.05$; **, $P < 0.01$). B and C, expression levels of CYP3A5 mRNA in 60 paired HCC and adjacent nontumor tissues were evaluated by qRT-PCR. D, the representative expression of CYP3A5 protein in tumor (T) and paired adjacent nontumor (N) tissues measured by Western blotting assay. E, comparison of CYP3A5 expression in 75 paired tumor tissues and adjacent nontumor tissues using IHC staining in HCC tissue microarray. F, representative images of IHC staining of CYP3A5 in differentiated (metastatic potential) HCC tissues from HCC tissue microarray. Comparison of CYP3A5 expression in HCC tissues was analyzed (*, $P < 0.05$). G, comparison of CYP3A5 expression in paired tumor tissues and the corresponding portal vein tumor thrombus (PVTT) by qRT-PCR.

that in para-tumor tissues (Fig. 1A). Similar results were also found in 68% (41/60) paired HCC and adjacent nontumor tissues from our own HCC tissue bank (Fig. 1B and C), which was confirmed with Western blotting analysis in another 16 patients (Fig. 1D). We next performed immunohistochemical (IHC) staining with a tissue microarray containing 75 pairs of HCC and nontumor tissues (Supplementary Fig. S1A) and elucidated that IHC scores of CYP3A5 were significantly lower in tumor tissues (Fig. 1E). Well-differentiated HCCs showed higher CYP3A5 expression, as compared with those in poorly differentiated HCCs samples (Fig. 1F). As shown in Supplementary Table S1, correlation regression analysis indicated that expression of CYP3A5 was negatively correlated with several malignant characteristics, in which the mRNA levels of CYP3A5 were significantly lower than their matched tumor tissues (Fig. 1G). Similarly, the relative lower expression of CYP3A5 was also observed in vascular invasion stable cell line CSQT-1 (Supplementary Fig. S1B). Together, these data indicated that CYP3A5 may play a protective role in the metastasis or invasion of HCC.

Published OnlineFirst February 3, 2015; DOI: 10.1158/0008-5472.CAN-14-1589

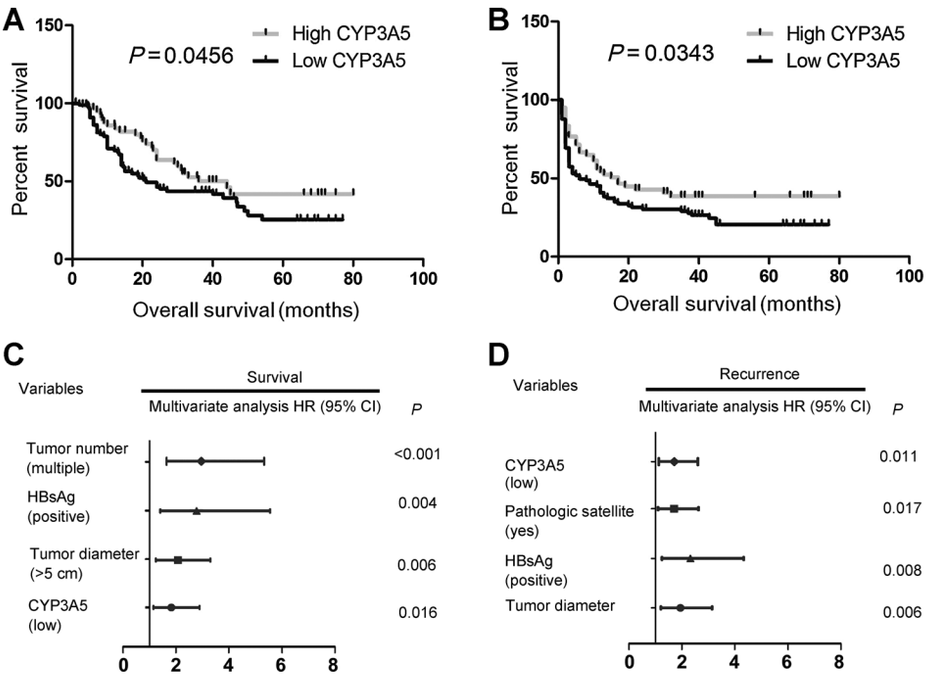

Figure 2.
Downregulated expression of CYP3A5 predicts poor prognosis in patients with HCC. A and B, the OS and TFS for the high and low CYP3A5 expression groups were analyzed by the two-sided long-rank test. C and D, a multivariate analysis of the HRs showed that the downregulation of CYP3A5 may be an independent prognostic factor for the OS and TFS rates (by the Cox multivariate proportional hazard regression model). The HRs are presented as the means (95% CI). The variables included in the multivariate analysis were selected using a univariate analysis.

Downregulated expression of CYP3A5 predicts poor prognosis in HCC patients

To further evaluate the significant contribution of CYP3A5 expression in the prognosis of patients with HCC, we applied another HCC tissue microarray with follow-up data containing 159 pairs of HCC and nontumor tissues (Supplementary Fig. S2A). The 159 patients with HCC were divided into two groups according to the CYP3A5 expression in tumors: a high CYP3A5 expression group ($n = 61$) and a low CYP3A5 expression group ($n = 98$). As shown in Fig. 2A and B, patients with higher CYP3A5 expression exhibited better overall survival (OS, median OS times were 44 vs. 21 months, respectively; difference = 23 months, $P < 0.05$) and tumor-free survival (TFS, median TFS times were 17 vs. 6 months, respectively; differences = 11 months, $P < 0.05$). The univariate and multivariate analysis further indicated that the CYP3A5 expression level was an independent risk factor for both OS and TFS for patients with HCC (Fig. 2C and D and Supplementary Tables S2 and S3). The group with the lower expression of CYP3A5 displayed shorter OS and TFS rates [OS: HR = 1.788; 95% CI, 1.113–2.872; $P = 0.016$; TFS: HR = 1.719, 95% CI, 1.132–2.610, $P = 0.011$]. Taken together, these data indicated that the expression level of CYP3A5 may be used as an independent factor for predicting the prognosis of HCC.

Ectopic expression of CYP3A5 ameliorates HCC migration and invasion, both *in vitro* and *in vivo*

We then used lentivirus encoding CYP3A5 to establish CYP3A5 stable cell lines with SMMC-7721 and HCCLM3 cells (named as SMMC-7721-CYP3A5 and HCCLM3-CYP3A5), which showed lower expression levels of endogenous CYP3A5 in eight HCC cell lines (Supplementary Fig. S3A). Transwell migration and Matrigel invasion assays revealed that exogenous expression of CYP3A5 dramatically inhibited cell migration and invasion in comparison with that of control cells (SMMC-7721-GFP, HCCLM3-GFP; Fig. 3A and B). As the adhesion capacity of tumor cells to the extracellular matrix (ECM) is a key step during tumor metastasis, we therefore performed cell adhesion assays with SMMC-7721-CYP3A5, HCCLM3-CYP3A5, and their respective control cells by using fibronectin-coated culture plate. As shown in Fig. 3C, forced expression of CYP3A5 significantly inhibited cell adhesion. In addition, cell growth analyses were also carried out by applying Cell Counting Kit-8 (CCK-8) assays and no significant differences were observed (Supplementary Fig. S3B).

We subsequently injected SMMC-7721-CYP3A5 and SMMC-7721-GFP cells into the lateral veins of the nude mice to verify the consequences of ectopic expression of CYP3A5 *in vivo*. Visual and microscopic evaluation of the metastatic growth in the lungs of the nude mice showed fewer and smaller foci in the presence of CYP3A5 ten weeks after injection (8 vs. 18 nodules per lung in SMMC-7721-CYP3A5 and control cells, respectively; Fig. 3D). Moreover, mice injected with SMMC-7721-CYP3A5 cells had a significantly higher survival rate (CYP3A5 group vs. GFP group: 50.0% vs. 9.1%, $P = 0.0286$, with 90 days as the cutoff; Fig. 3E). Collectively, these results indicated that CYP3A5 is capable of manipulating aggressive and metastatic phenotype of HCC both *in vitro* and *in vivo*.

CYP3A5 induces expression of TIMP1 and TIMP2 by inhibiting AKT signaling

To investigate the underlying molecular mechanisms of the CYP3A5-mediated attenuation of HCC metastasis, we firstly identified the potential regulation of CYP3A5 on the epithelial–mesenchymal transition (EMT), which is considered to be a key process of cancer metastasis. As shown in Fig. 4A, no significant differences of EMT-related genes, such as E-cadherin, N-cadherin, vimentin, and Snail, were observed upon CYP3A5

Published OnlineFirst February 3, 2015; DOI: 10.1158/0008-5472.CAN-14-1589

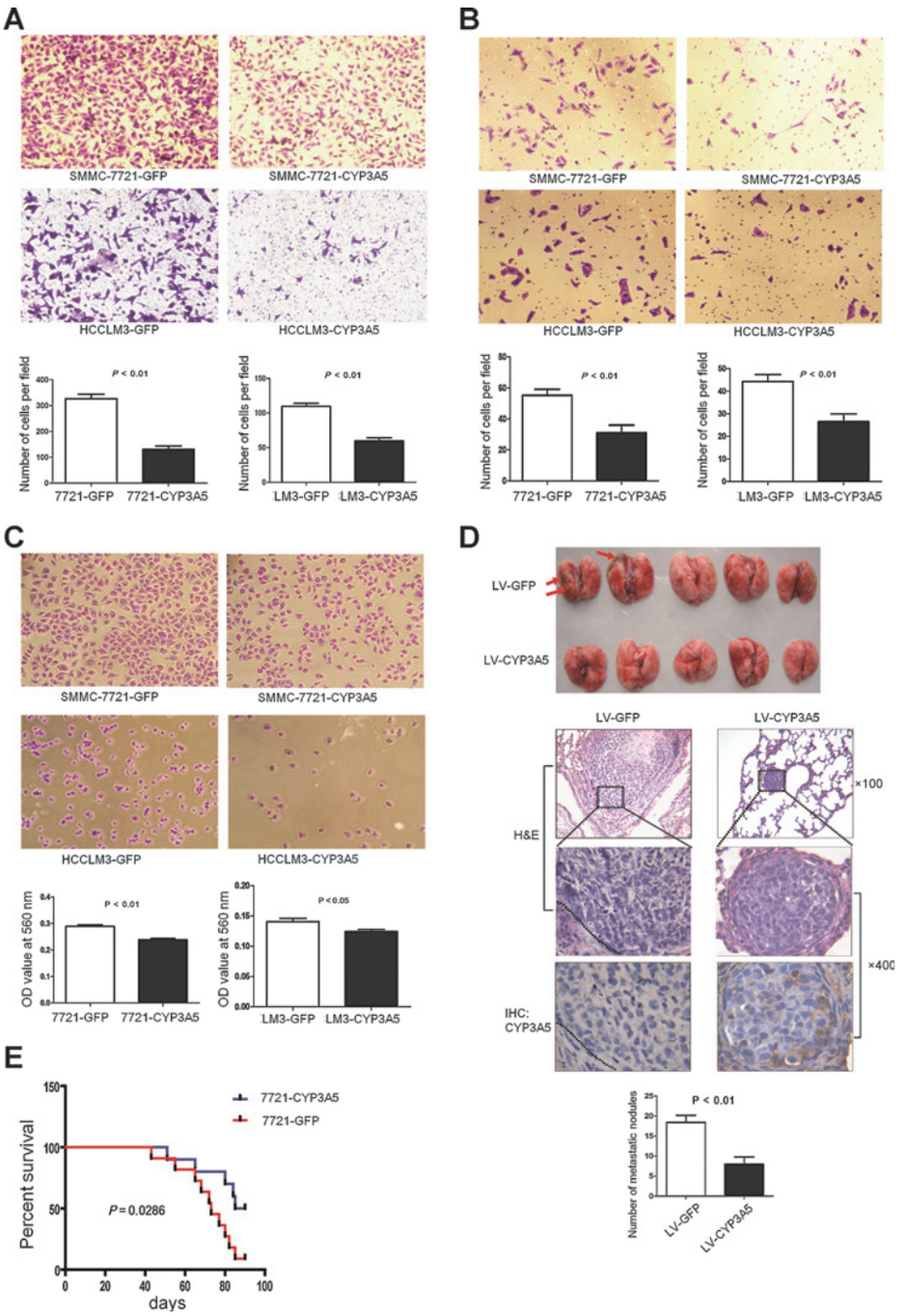

Figure 3.
Ectopic expression of CYP3A5 ameliorates HCC migration and invasion, both *in vitro* and *in vivo*. A, cell migration assays of SMMC-7721-CYP3A5, HCCLM3-CYP3A5, and the respective control cells were performed utilizing polycarbonate membrane inserts in 24-well plate. Representative images are shown. Magnification, ×200. The results were plotted as the average number of migrated cells from six random microscopic fields. Three independent experiments were performed and the similar results were obtained. B, cell invasion assays of SMMC-7721-CYP3A5, HCCLM3-CYP3A5, and the respective control cells were performed using BioCoat Matrigel invasion chambers in 24-well plate. Representative images are shown. Magnification, ×200. The results were plotted as the average number of invasive cells from six random microscopic fields. Three independent experiments were performed and the similar results were obtained. C, cell adhesion assays of SMMC-7721-CYP3A5, HCCLM3-CYP3A5, and the respective control cells were analyzed using a CytoSelectTM 48-Well Adhesion Assay Kit. Representative images are shown. Magnification, ×200. The results were plotted as the average OD value at 560 nm. Three independent experiments were performed and the similar results were obtained. D, representative image of the visible metastatic nodules in the mouse lungs of the SMMC-7721-GFP group and the SMMC-7721-CYP3A5 group ($n = 5$, top). Representative hematoxylin and eosin (H&E) images of metastatic nodules from the mouse lung tissue sections of the SMMC-7721-GFP group and the SMMC-7721-CYP3A5 group (middle). The number of metastatic nodules in the lungs of each group was presented as the mean ± SD (bottom). E, OS curves for the two groups of nude mice injected with either SMMC-7721-GFP or SMMC-7721-CYP3A5 through the lateral tail veins ($n = 10$). *P* value was calculated using the two-sided log-rank test.

expression, indicating that CYP3A5-mediated attenuation of HCC metastasis was EMT independent. MMPs are proteolytic enzymes that can degrade ECM components. Recently, certain aspects of MMPs involvement in tumor metastasis such as tumor-induced angiogenesis, tumor invasion, and establishment of metastatic foci at the secondary site have received extensive attention that resulted in an overwhelming amount of experimental and observational data in favor of critical roles of MMPs in these processes (12). Interestingly, we observed the remarkable increase of TIMP1 and TIMP2 expression in both SMMC7721-CYP3A5 and HCCLM3-CYP3A5 cells, whereas no differences were found in the expression of MMP2, 7, or 9 (Fig. 4B). As expected, a zymography assay further revealed that the activities of MMP2 and 9 were dramatically inhibited in CYP3A5-overexpressed cells (Fig. 4C).

Moreover, after treatment with HGF or EGF, p-AKT was clearly inactivated in the presence of CYP3A5, whereas p-ERK, p-JNK, and p-P38 revealed no such changes (Fig. 4D and Supplementary Fig.

Published OnlineFirst February 3, 2015; DOI: 10.1158/0008-5472.CAN-14-1589

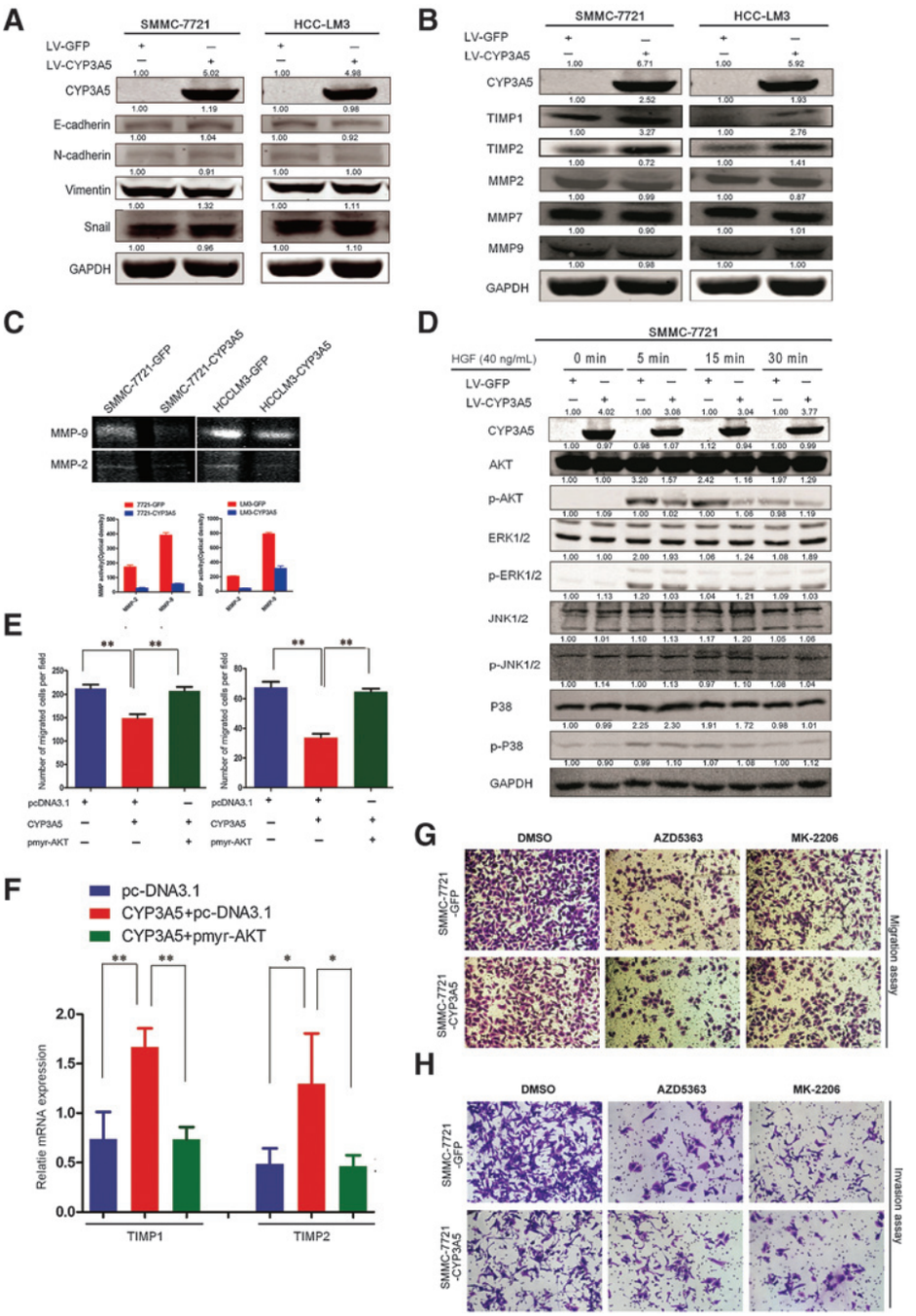

Figure 4.
CYP3A5 induces expression of TIMP1 and TIMP2 by inhibiting AKT signaling. A, the expression levels of E-cadherin, N-cadherin, vimentin, and Snail were compared by Western blotting analysis between the indicated cell lysates. B, TIMP1, TIMP2, MMP2, MMP7, and MMP9 expression levels were measured by Western blotting in the indicated cell lysates. C, the activities of MMP2 and MMP9 were detected by the zymography assay. The bottom histogram shows the average optical density from three repeated experiments. D, the SMMC-7721 cells were starved with serum-free DMEM overnight and exposed to HGF (40 ng/mL) for 0, 5, 15, and 30 minutes. The total expression levels and phosphorylation levels of AKT (p-AKT), ERK1/2 (p-ERK1/2), JNK1/2 (p-JNK1/2), and P38 (p-P38) were analyzed by Western blotting. E, SMMC-7721 cells were transiently transfected with a control vector (pcDNA3.1), or pcDNA-CYP3A5, or pcDNA-CYP3A5 plus pmyr-AKT. The cells were subjected to the Transwell migration assay and the Matrigel invasion assay after 24 hours of transfection. The results were plotted as the average number of migrated (left, bottom) or invasive (right, bottom) cells from six random microscopic fields (**, $P < 0.01$). Representative images are shown in Supplementary Fig. S4C. F, the relative expression levels of TIMP1 and TIMP2 were analyzed by qRT-PCR after 48 hours of transfection indicated as D (*, $P < 0.05$; **, $P < 0.01$). Three independent experiments were performed. G and H, two stable cell lines, SMMC-7721-GFP and SMMC-7721-CYP3A5, were treated with AKT inhibitors, AZD5363 (10 μmol/L) or MK-2206 (2 μmol/L), and then the capacity of cell migration (G) or invasion (H) was examined.

S4A and S4B). To further study whether the AKT signaling pathway was necessary for CYP3A5-mediated suppression of HCC metastasis, we transiently transfected SMMC-7721 cells with full-length CYP3A5 plasmid (pcDNA3.1-CYP3A5) and pmyr-AKT (dominant-active AKT) or pcDNA3.1-CYP3A5 alone. As shown in Fig. 4E and Supplementary Fig. S4C and S4F, we noticed that cell migration and invasion were inhibited in couple with increased expression of TIMP1 and TIMP2 in the presence of CYP3A5, whereas such changes were mostly reversed in pcDNA3.1-CYP3A5 and pmyr-AKT cotransfection group. In addition, two specific AKT inhibitors (Supplementary Fig. S5A), AZD5363 and MK2206, were applied to further verify whether low CYP3A5 cells are more susceptible to migration and invasion inhibition. As shown in Fig. 4G and H and Supplementary Fig. S5, the migration and invasion capability were remarkably attenuated upon AKT inhibitor treatment in both SMMC-7721-GFP and HCCLM3-GFP cells, whereas no obvious differences were observed in SMMC-7721-CYP3A5 or HCCLM3-CYP3A5 cells. Together, these data suggest that intracellular PI3K-AKT–dependent proteolytic enzymes signaling, but not the MAPK signal

Published OnlineFirst February 3, 2015; DOI: 10.1158/0008-5472.CAN-14-1589

pathway, may play the key role in the modulation of CYP3A5-involved HCC metastasis.

CYP3A5 selectively inhibits AKT phosphorylation at Ser473 by blocking mTORC2 kinase activity

It has been documented that phosphorylations of both Thr308 and Ser473 residues contribute to the full activation of AKT (13). Thr308 is phosphorylated by PDK1, whereas other candidates, including mTORC2, may perform the AKT phosphorylation at Ser473 (14). We therefore examined the change of p-AKT (S473) and p-AKT (T308) in SMMC-7721-CYP3A5 and the control cells following HGF stimulation. Western blotting analysis revealed no obvious differences of p-AKT (T308) between CYP3A5 and the control cells. Importantly, the level of p-AKT (S473) triggered by HGF stimulation significantly decreased in CYP3A5-expressing cells (Fig. 5A). Clinically, the inverse correlation between the levels of CYP3A5 and p-AKT (S473) were observed in 159 pairs of HCC specimens we previously applied (Supplementary Fig. S5E). In addition, no changes were observed on the upstream regulators of p-AKT (T308), including P85 (regulatory subunit of PI3K), PTEN, and PDK1 between CYP3A5-overexpressing and control cells (Fig. 5B), indicating the selective inhibition of p-AKT (S473) and mTORC2 might be necessary for CYP3A5-mediated physiologic function.

Next, we transfected synthesized siRNA specifically targeting Rictor, the indispensible component of mTORC2 (14), into SMMC-7721-GFP and SMMC-7721-CYP3A5 cell lines (Fig. 5C), and found that silencing of Rictor abrogated the difference of p-AKT (S473) between the CYP3A5-overexpressing and control cells (Fig. 5D). Furthermore, we evaluated the effect of mTORC2 knockdown on the metastatic phenotype of HCC cell lines by utilizing Transwell migration and Matrigel invasion assays. As expected, migration and invasion capacities of both SMMC-7721-GFP and SMMC-7721-CYP3A5 cell lines ameliorated to similar levels upon Rictor siRNA treatment (Fig. 5E and F and Supplementary Fig. S6A and S6B). It has been reported that the complex formation of mTORC2 and mTORC2 kinase activity were responsible for the phosphorylation of AKT (S473), we therefore performed an immunoprecipitation assay using antibody against Rictor to check mTORC2 complex formation and *in vitro* mTORC2 kinase activity between CYP3A5-overexpressing and its control cells. Interestingly, no obvious changes were observed in the total amount of key components (mTOR and Rictor) of mTORC2 complex upon HGF stimulation; nevertheless, the *in vitro* mTORC2 kinase activity in SMMC-7721-CYP3A5 cells was markedly decreased (Fig. 5G). As previous study demonstrated that phosphatidic acid was required for the stabilization of the mTORC2 complex (15), we thus attempted to assess phosphatidic acid contents in SMMC-7721-CYP3A5, HCCLM3-CYP3A5, and their counterpart control cell lines. No significant differences of phosphatidic acid levels were found between CYP3A5-overexpressing and their control cells (Supplementary Fig. S6C), supporting the observation that the integrity of the mTORC2 complex is not responsible for CYP3A5 function.

These data revealed that CYP3A5 exerts its physiologic function through modulating mTORC2 kinase activity rather than the stability of the mTORC2 complex, which in turn results in the dephosphorylation of AKT on S473 and elevated expression of TIMPs.

CYP3A5-induced intracellular ROS enrichment is responsible for the regulation of mTORC2/p-AKT (S473) signaling

CYP3A5, a kind of mitochondrial P450 type enzymes, catalyzes central steps in steroid biosynthesis. These mono-oxygenase reactions depend on electron transfer from NADPH via FAD adrenodoxin reductase and 2Fe-2S adrenodoxin (16–18). These systems can function as a futile NADPH oxidase, oxidizing NADPH in absence of substrate, and leak electrons via adrenodoxin and P450 to O_2, producing superoxide and other ROS (16–18). Here, increased level of intracellular ROS was observed in both SMMC-7721-CYP3A5 and HCCLM3-CYP3A5 cells in comparison with their counterpart control cells (Fig. 6A and B). In addition, Supplementary Fig. S7A–S7C showed that pretreatment of CYP3A5-overexpressing cells with DPI, a potent inhibitor of flavonoid-containing enzymes such as NADPH oxidase and nitric oxide synthase, completely abolished the induction of ROS production and enhanced the level of AKT phosphorylation (S473), indicating a potential role for NADPH oxidase in CYP3A5/ROS-regulated AKT activity.

As expected, the loss of migration capacity and intracellular AKT phosphorylation in CYP3A5 stable cells was notably enhanced to the similar level in control cells upon the induction of N-acetylcysteine (NAC; Fig. 6C and D). To further verify whether enrichment of ROS is responsible for CYP3A5-regulated mTORC2 kinase activity and AKT signaling, we firstly treated cells with 100 μmol/L H_2O_2, and found that both mTORC2 kinase activity and AKT phosphorylation (S473) were dramatically decreased, which were restored again followed with antioxidant treatment (Fig. 6E). This result indicated that ROS could negatively regulate mTORC2 kinase activity *in vitro*. Next, CYP3A5 stable and respective control cells were pretreated with either of antioxidants (NAC or GSH) for 3 hours and stimulated with HGF. As shown in Fig. 6F, the treatment of antioxidant resulted in the restoration of mTORC2 kinase activity in CYP3A5 cells. As previously reported that mTORC2–Ribosome interaction is necessary for mTORC2-induced AKT activation (19), we examined whether the treatment of HGF may lead to the assembly of the mTORC2–ribosome complex. The immunoprecipitation assay showed the augment of Rictor or mTOR and ribosomal protein Rpl26 (Supplementary Fig. S7D) with the induction of HGF. Importantly, the stability of the Rictor/Rpl26 and mTOR/Rpl26 complexes was disrupted in the presence of H_2O_2 (Fig. 6G). Together, with the observation that knockdown of Rpl7 decreased HGF-stimulated phosphorylation of AKT in control cells to the similar level as CYP3A5-expressing cells did (Supplementary Fig. S7E), these data revealed that CYP3A5-induced intracellular ROS accumulation may play the key factor for the regulation of mTORC2–ribosome interaction, mTORC2 kinase activity, and mTORC2/p-AKT (S473) signaling. As an important supporting evidence, the GSH/GSSG ratio, which are negatively correlated with ROS level (16–18), in clinical HCC samples ($n = 62$, 31 with microvascular invasion named as HM tissues, 31 without microvascular invasion named as LM tissues) were measured and found the remarkably lower GSH/GSSG level in the LM group (Fig. 6H).

Discussion

CYP3A5, a member of the cytochrome P450 superfamily of enzymes, is involved in the metabolism of drugs, exogenous carcinogens, and endogenous molecules such as steroids (20). Previous studies about CYP3A5 have mainly focused on two

Published OnlineFirst February 3, 2015; DOI: 10.1158/0008-5472.CAN-14-1589

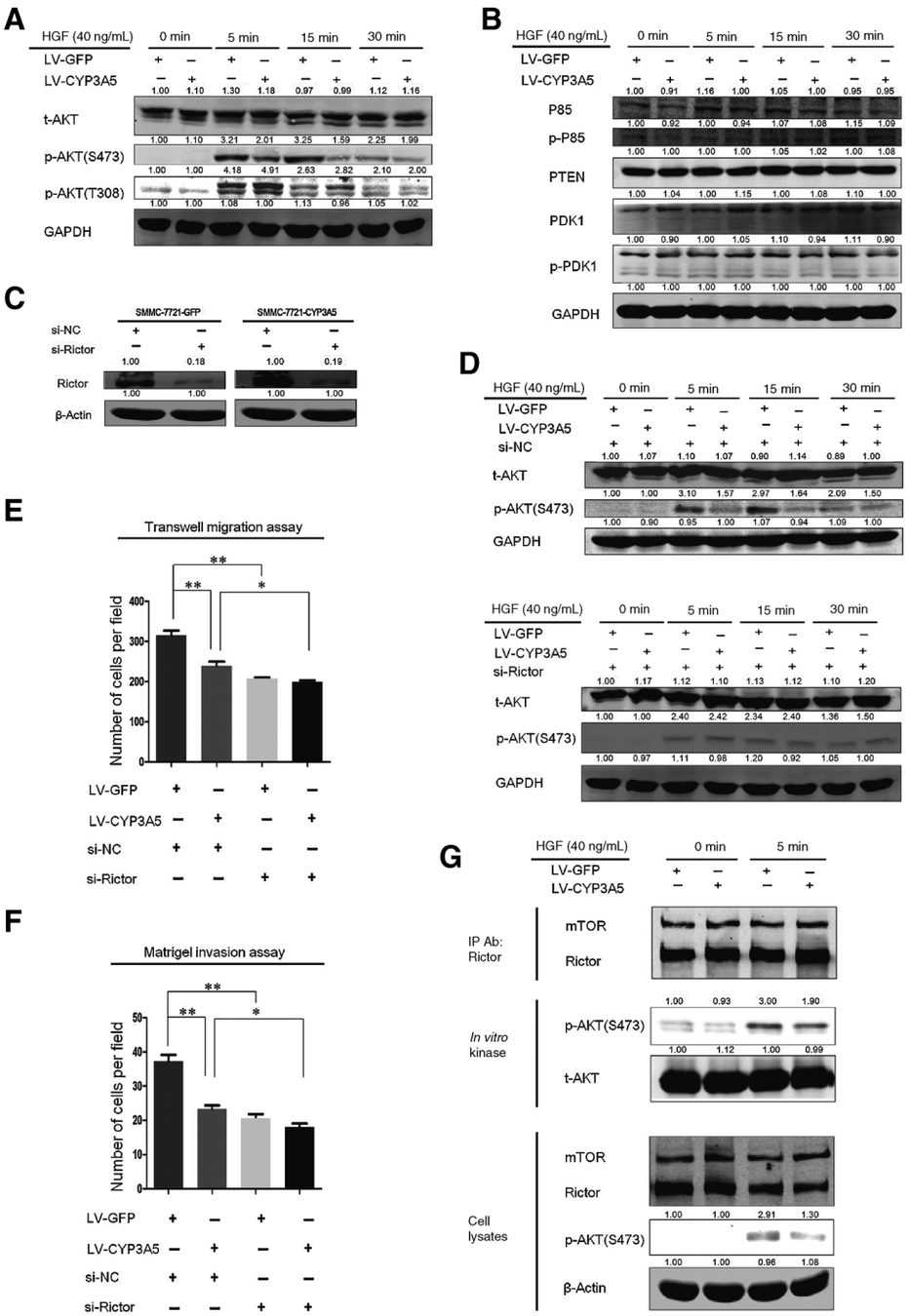

Figure 5.

CYP3A5 selectively inhibits AKT phosphorylation at Ser473 by blocking mTORC2 kinase activity. A and B, SMMC-7721-GFP and SMMC-7721-CYP3A5 cell lines were serum-starved overnight and then stimulated with HGF (40 ng/mL) for indicated time periods. A, the total expression of AKT (t-AKT) and phosphorylation levels of AKT, including p-AKT (S473) and p-AKT (T308), were analyzed by Western blotting. B, the major upstream regulators of p-AKT (T308) were probed by Western blotting with indicated antibodies. C, SMMC-7721-GFP and SMMC-7721-CYP3A5 cells were transfected with siRNA duplexes targeted against human Rictor (si-Rictor) or control siRNA (si-NC). Forty-eight hours after transfection, the knockdown efficiency was evaluated by the Western blotting assay. D, SMMC-7721-GFP and SMMC-7721-CYP3A5 cell lines were transfected with siRNA duplexes targeted against human Rictor (si-Rictor) or control siRNA (si-NC). The cells were serum-free starved overnight and subjected to HGF (40 ng/mL) for indicated time periods after 48 hours of transfection. The cell lysates were analyzed by Western blotting with anti-AKT, anti-AKT (S473), and anti-GAPDH antibodies. E and F, SMMC-7721-GFP and SMMC-7721-CYP3A5 cell lines were transfected with siRNA duplexes targeted against human Rictor (si-Rictor) or control siRNA (si-NC). Forty-eight hours after transfection, the indicated cell lines were subjected to the Transwell migration assay (D) and the Matrigel invasion assay (E). The results were plotted as the average number of migrated (invasive) cells from six random microscopic fields (*, $P < 0.05$; **, $P < 0.01$). Three independent experiments were performed and the similar results were obtained. G, SMMC-7721-GFP and SMMC-7721-CYP3A5 cell lines were serum-starved overnight and then exposed to HGF (40 ng/mL) for 0 and 5 minutes. The cells were lysed in CHAPS buffer and immunoprecipitations (IP) were performed using anti-Rictor antibody. *In vitro* mTORC2 kinase assays were performed utilizing inactive AKT1 as a substrate of anti-Rictor immunoprecipitates. Immunoprecipitates and cell lysates were subjected to Western blotting analysis using anti-mTOR, anti-Rictor, anti-p-AKT (S473), and anti-β-Actin antibodies.

Published OnlineFirst February 3, 2015; DOI: 10.1158/0008-5472.CAN-14-1589

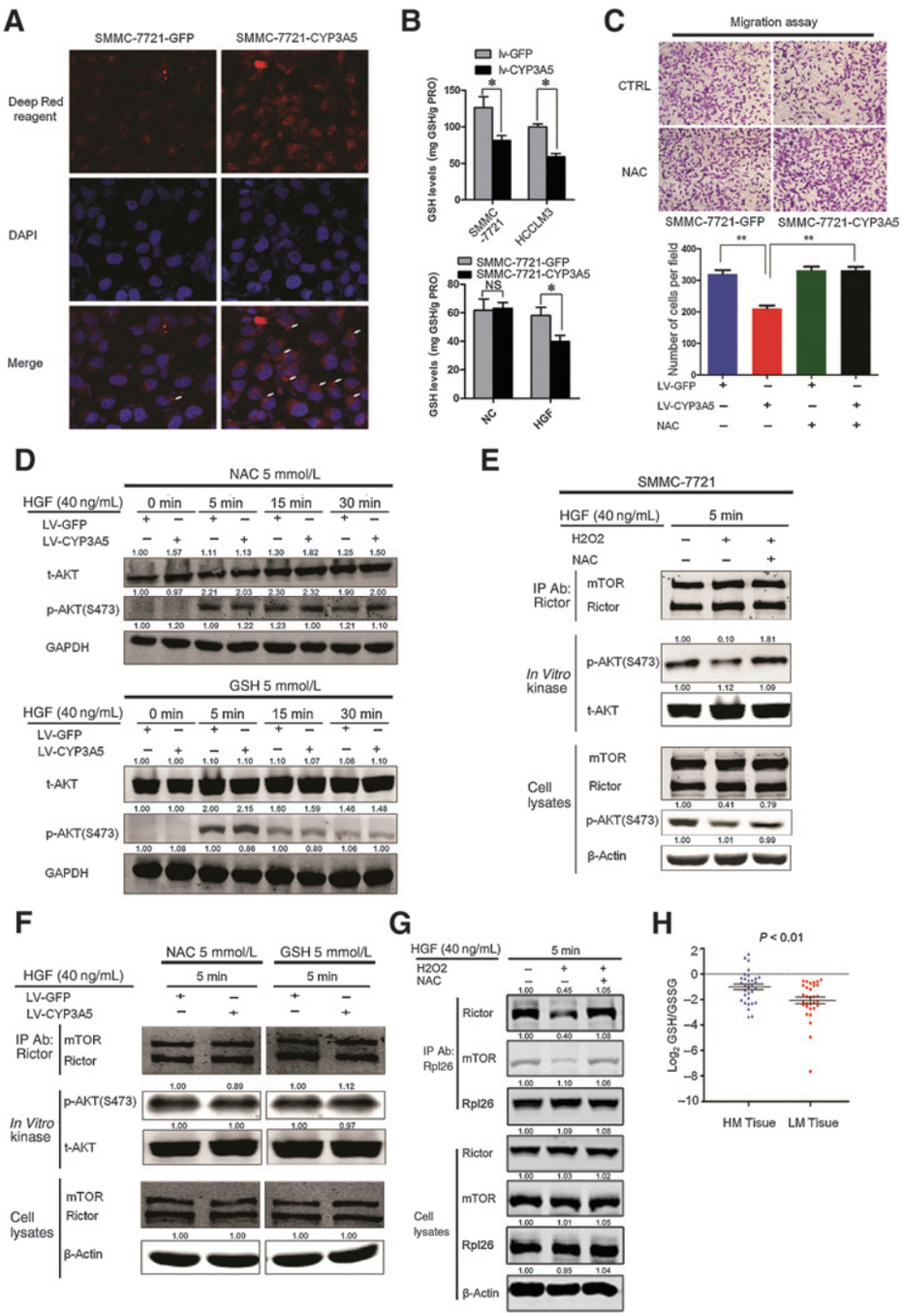

Figure 6.

CYP3A5-induced intracellular ROS enrichment is responsible for the regulation of mTORC2/p-AKT (S473) signaling. A, SMMC-7721-GFP and SMMC-7721-CYP3A5 cell lines were serum-starved overnight and then exposed to HGF (40 ng/mL) for 5 minutes. Intracellular ROS levels of indicated cell lines were measured using CellROX Deep Red Reagent. The fluorescent images were captured using a confocal microscope. White arrows, the dots for ROS staining. Magnification, ×600. B, the intracellular GSH level was examined. Top, the GSH content in SMMC-7721-CYP3A5 and HCCLM3-CYP3A5 versus SMMC-7721-GFP and HCCLM3-GFP cell lines was measured with DMEM medium containing 10% FBS; we calculated the GSH level of serum-starved SMMC-7721-CYP3A5 and GFP cells in the absence or presence of HGF stimulation (bottom). Three independent experiments were performed (*, $P < 0.05$). C, SMMC-7721-GFP and SMMC-7721-CYP3A5 cells were preconditioned with or without NAC (5 mmol/L) for 3 hours, and then subjected to Transwell migration assays. Representative images are shown (top). Magnification, ×200; The results are plotted as the average number of migrated cells from six random microscopic fields (bottom). Three independent experiments were performed (**, $P < 0.01$). D, indicated cell lines were starved with serum-free DMEM medium overnight and pretreated with the antioxidant NAC (5 mmol/L) or GSH (5 mmol/L) for 3 hours. Then the cells were exposed to HGF (40 ng/mL) for 5 minutes and lysed in CHAPS buffer. *In vitro* mTORC2 kinase assays and immunoprecipitations were performed using anti-Rictor antibody. E, SMMC-7721 cell lines were serum-starved overnight and pretreated with or without H_2O_2 (100 μmol/L) for 30 minutes before HGF (40 ng/mL) stimulation. (*Continued on the following page.*)

Published OnlineFirst February 3, 2015; DOI: 10.1158/0008-5472.CAN-14-1589

major aspects, the potential relationship of CYP3A5 polymorphism and cancer risk or drug metabolism (9–11, 21–26). Moreover, Tsunedomi R concluded that the expression of CYP3A5 was drastically decreased in conjunction with venous invasion and might serve as a marker of progression and molecular target for treatment of HCV-associated HCC (27). Similar findings were also reported in some earlier articles (28, 29). Importantly, the expression of CYP3A5 was declined from early to late hepatic cirrhosis. In our current study, CYP3A5 expression was found frequently downregulated in tumor tissues and was negatively associated with several malignant characteristics and poor prognosis in patients with HCC. Ectopic expression of CYP3A5 attenuated cell migration, invasion, and cell–ECM adhesion both *in vitro* and *in vivo*. To our knowledge, this is the first study that intensively evaluates the protective effects of CYP3A5 on HCC progression, besides its enzyme activity.

In addition, we also examined the role of CYP3A4 in HCC progression. In line with previous studies, CYP3A4 showed lower expression level in most of tumor tissues, which was significantly correlated with differentiation grade, tumor number, and TNM (Supplementary Fig. S8A–S8C). Because of the relative high expression level of CYP3A4 across eight HCC cell lines we used in Supplementary Fig. S3, we explored the effect of CYP3A4 on HCC cells by using RNAi method (Supplementary Fig. S8D). A slightly decreased growth rate was observed in SMMC-7721-Si-CYP3A4 ($P > 0.05$) but not HCCLM3-Si-CYP3A4 cells in comparison with their matched control cells. Furthermore, no obvious changes of ROS accumulation, cell migration, and invasion were found between CYP3A4-knockdown and control cells (Supplementary Fig. S8E–S8G). These data reinforced the protective effects of CYP3A5 but not CYP3A4 in regulating HCC metastasis. The primary role of CYP3A5 for ROS-attenuated AKT signaling might result from (i) the relatively saturated level of CYP3A4 in HCC cells that might weaken the effect of the RNAi assay; and (ii) a possible selective mechanism for ROS accumulation in response to CYP3A5 expression.

mTOR belongs to the PI3K-related protein kinase subfamily that plays a pivotal role in the regulation of various cellular processes, including cell growth, migration, and cell metabolism (30). mTOR consists of two distinct complexes, termed mTORC1 and mTORC2, which have slight differences in the subunit compositions (30, 31). Specifically, mTORC1 consists of five components, mTOR, Raptor, mLST8/GβL, PRAS40, and DEPTOR (30, 31); mTORC2 is composed of six components, including mTOR, Rictor, mLST8/GβL, DEPTOR, PROTOR/PRR5 (proline-rich protein 5), and mSIN1 (14, 31). Rictor controls the stability of the mTORC2 complex (14, 32). mTORC2 is primarily activated by growth factors despite its underlying mechanism remaining largely unknown (16). AKT is an important kinase mediating survival signaling, which is regulated by phosphorylation on Thr308 by PDK1 and on Ser473 by several other kinases, as well as mTORC2 (33). In the current study, p-AKT (S473) was obviously inactivated in CYP3A5 stable cells; nevertheless, p-AKT (T308) presented no significant difference. The phosphorylation of AKT (S473) was strongly repressed to similar levels between CYP3A5-overexpressing and control cells in response to si-Rictor treatment. We thus speculated that CYP3A5-blocked p-AKT (S473) activity might depend on the mTORC2 activity. Consistently, there were no significant differences in metastatic phenotypes between SMMC-7721-CYP3A5 and SMMC-7721-GFP cells following Rictor silencing. Several published studies have demonstrated that downregulation of the mTORC2 kinase activity usually resulted from the dissociation of the mTORC2 complex (15, 34–36). More importantly, the novel finding in our current study was that CYP3A5-mediated inactivation of p-AKT (S473) resulted from the inhibition of mTORC2 kinase activity, rather than disruption of the mTORC2 complex.

Although multiple endogenous and exogenous substances have been reported to be involved in regulation of mTORC2 activity (15, 33–38), second messengers, for instance ROS, regulating mTORC2 remains less well understood. Structural and biochemical characterization studies conducted on TOR (the yeast ortholog of mTOR) reveal that, owing to the presence of a redox-sensitive motif, the cellular stability or functionality of TOR is redox regulated (39). Consistent with this finding, several studies demonstrated the ability of ROS to regulate the functional activity of mTORC1 (40, 41). Of special interest is that ROS were also reported to facilitate or oppositely suppress mTORC2 activity in newly emerging evidences (42, 43). Supporting evidence was obtained recently that ROS generation in response to a DNA alkylating agent inhibit mTORC2 activity by affecting the complex assembly (44). It seemed that ROS were double-edged swords in the regulation of mTORC2 activity. ROS at high levels become deleterious, exhibiting pathophysiologic actions, whereas, at low levels, they may be benefit for normal physiologic actions (45–47), which is called "ROS threshold concept" (46, 47).

In our current study, the HCC cells benefited from exposure to CYP3A5-mediated ROS generation, and therefore exerted attenuation of metastasis. Mechanically, the ROS level in CYP3A5-overexpressing cells dramatically suppressed the mTORC2 activity, without affecting the mTOR/Rictor complex assembly. We considered that the level of CYP3A5-induced intracellular ROS was within a certain threshold value. Hydrogen peroxide (H_2O_2) represents an important type of ROS and certain concentrations (5–200 μmol/L) of H_2O_2 have been proven to induce an appropriate amount of ROS production within the ROS threshold in multiple cell lines (48). Thus 100 μmol/L H_2O_2 was applied in our study to simulate the elevated intracellular ROS level in HCC cells. Moreover, it seemed that supplementation of antioxidants achieved unexpected promotion instead of inhibition of metastatic phenotype in our study. Therefore, it might be harmful to supply exogenous antioxidants in the presence of CYP3A5-mediated ROS production despite their fundamental role of antioxidants in human life and health.

(*Continued.*) Indicated cells were exposed to the antioxidant NAC (5 mmol/L) for 3 hours before harvesting. The cells were lysed and immunoprecipitations were performed using anti-Rictor antibody. *In vitro* mTORC2 kinase assay containing anti-Rictor immunoprecipitates and inactive AKT1 was performed. Immunoprecipitates and cell lysates were then subjected to Western blotting and probed with the indicated antibodies. F, indicated cell lines were starved overnight and pretreated with NAC (5 mmol/L) or GSH (5 mmol/L) for 3 hours before HGF (40 ng/mL) stimulation. The cells were harvested at corresponding time point and subjected to Western blotting with indicated antibodies. G, the cells were lysed and immunoprecipitation were performed using anti-Rpl26 antibody. Cell lysates were then subjected to Western blotting and probed with the indicated antibodies. H, GSH/GSSG contents in clinical HCC samples with higher (HM, $n = 31$) or lower (LM, $n = 31$) metastatic capacity were measured and compared.

Published OnlineFirst February 3, 2015; DOI: 10.1158/0008-5472.CAN-14-1589

In the current study, our results reveal that CYP3A5 plays an important protective role in HCC metastasis, independent of the activation of carcinogens and metabolism of anticancer drugs. Forced expression of CYP3A5 in HCC cells inhibits cell migration and invasion *in vitro* and *in vivo*, at least partly via manipulating ROS/mTORC2/p-AKT (S473) signaling, which provides a potential marker for cancer prevention and treatment.

Disclosure of Potential Conflicts of Interest

No potential conflicts of interest were disclosed.

Authors' Contributions

Conception and design: F. Jiang, L. Chen, Y.-C. Yang, H.-Y. Wang
Development of methodology: F. Jiang, Y.-C. Yang, R.-Y. Wang, L. Li, C.-Y. Chen
Acquisition of data (provided animals, acquired and managed patients, provided facilities, etc.): F. Jiang, Y.-C. Yang, R.-Y. Wang, Y.-X. Chang
Analysis and interpretation of data (e.g., statistical analysis, biostatistics, computational analysis): F. Jiang, L. Chen, Y.-C. Yang, L. Li, W.-T. Huang, H.-Y. Wang
Writing, review, and/or revision of the manuscript: F. Jiang, L. Chen, Y.-C. Yang, H.-Y. Wang
Administrative, technical, or material support (i.e., reporting or organizing data, constructing databases): Y.-C. Yang, X.-M. Wang, W. Wen, G.-M.-Y. Liu, W.-T. Huang
Study supervision: L. Chen, J. Tang, G.-M.-Y. Liu, L. Xu, H.-Y. Wang

Acknowledgments

The authors thank Dong-Ping Hu, Shan-Hua Tang, Lin-Na Guo, Dan Cao, Dan-Dan Huang, and Shan-Na Huang for technical assistance.

Grant Support

This work was supported by Chinese Key Project for Infectious Diseases (2012ZX10002), the National Basic Research Program of China (2012CB316503), Science Fund from NSFC, China (30921006,81201940,81422032,81472702), Chinese Postdoctoral Scientific Funding (2012M521859), Shanghai Young Scholarship Foundation (XYQ2013076), and Natural Science Foundation of Jiangsu Province, China (BK2012482).

The costs of publication of this article were defrayed in part by the payment of page charges. This article must therefore be hereby marked *advertisement* in accordance with 18 U.S.C. Section 1734 solely to indicate this fact.

Received June 4, 2014; revised December 8, 2014; accepted December 13, 2014; published OnlineFirst February 3, 2015.

References

1. Gonzalez FJ, Gelboin HV. Role of human cytochromes P450 in the metabolic activation of chemical carcinogens and toxins. Drug Metab Rev 1994;26:165–83.
2. Koehl W, Amin S, Staretz ME, Ueng YF, Yamazaki H, Tateishi T, et al. Metabolism of 5-methylchrysene and 6-methylchrysene by human hepatic and pulmonary cytochrome P450 enzymes. Cancer Res 1996;56:316–24.
3. Zhou SF. Drugs behave as substrates, inhibitors and inducers of human cytochrome P450 3A4. Curr Drug Metab 2008;9:310–22.
4. Windmill KF, McKinnon RA, Zhu X, Gaedigk A, Grant DM, McManus ME. The role of xenobiotic metabolizing enzymes in arylamine toxicity and carcinogenesis: functional and localization studies. Mutat Res 1997;376:153–60.
5. Mas VR, Maluf DG, Stravitz R, Dumur CI, Clark B, Rodgers C, et al. Hepatocellular carcinoma in HCV-infected patients awaiting liver transplantation: genes involved in tumor progression. Liver Transpl 2004;10:607–20.
6. Oguro A, Sakamoto K, Funae Y, Imaoka S. Overexpression of CYP3A4, but not of CYP2D6, promotes hypoxic response and cell growth of Hep3B cells. Drug Metab Pharmacokinet 2011;26:407–15.
7. Mitra R, Guo Z, Milani M, Mesaros C, Rodriguez M, Nguyen J, et al. CYP3A4 mediates growth of estrogen receptor-positive breast cancer cells in part by inducing nuclear translocation of phospho-Stat3 through biosynthesis of (±)-14,15-epoxyeicosatrienoic acid (EET). J Biol Chem 2011;286:17543–59.
8. Lamba JK, Lin YS, Schuetz EG, Thummel KE. Genetic contribution to variable human CYP3A-mediated metabolism. Adv Drug Deliv Rev 2002;54:1271–94.
9. Gellner K, Eiselt R, Hustert E, Arnold H, Koch I, Haberl M, et al. Genomic organization of the human CYP3A locus: identification of a new, inducible CYP3A gene. Pharmacogenetics 2001;11:111–21.
10. Wojnowski L. Genetics of the variable expression of CYP3A in humans. Ther Drug Monit 2004;26:192–9.
11. Lee SJ, Usmani KA, Chanas B, Ghanayem B, Xi T, Hodgson E, et al. Genetic findings and functional studies of human CYP3A5 single nucleotide polymorphisms in different ethnic groups. Pharmacogenetics 2003;13:461–72.
12. Deryugina EI, Quigley JP. Matrix metalloproteinases and tumor metastasis. Cancer Metastasis Rev 2006;25:9–34.
13. Scheid MP, Marignani PA, Woodgett JR. Multiple phosphoinositide 3-kinase-dependent steps in activation of protein kinase B. Mol Cell Biol 2002;22:6247–60
14. Guertin DA, Stevens DM, Saitoh M, Kinkel S, Crosby K, Sheen JH, et al. mTOR complex2 is required for the development of prostate cancer induced by Pten loss in mice. Cancer Cell 2009;15:148–59.
15. Toschi A, Lee E, Xu L, Garcia A, Gadir N, Foster DA. Regulation of mTORC1 and mTORC2 complex assembly by phosphatidic acid: competition with rapamycin. Mol Cell Biol 2009;29:1411–20.
16. Sun X, Ai M, Wang Y, Shen S, Gu Y, Jin Y, et al. Selective induction of tumor cell apoptosis by a novel P450-mediated reactive oxygen species (ROS) inducer methyl 3-(4-nitrophenyl) propiolate. J Biol Chem 2013;288:8826–37.
17. Hanukoglu I. Antioxidant protective mechanisms against reactive oxygen species (ROS) generated by mitochondrial P450 systems in steroidogenic cells. Drug Metab Rev 2006;38:171–96.
18. Priyadarsini RV, Nagini S. Quercetin suppresses cytochrome P450 mediated ROS generation and NF-κB activation to inhibit the development of 7,12-dimethylbenz anthracene (DMBA) induced hamster buccal pouch carcinomas. Free Radic Res 2012;46:41–9.
19. Zinzalla V, Stracka D, Oppliger W, Hall MN. Activation of mTORC2 by association with the ribosome. Cell 2011;144:757–68.
20. Nebert DW, Dalton TP. The role of cytochrome p450 enzymes in endogenous signalling pathways and environmental carcinogenesis. Nat Rev Cancer 2006;6:947–60.
21. Daly AK. Significance of the minor cytochrome P450 3A isoforms. Clin Pharmacokinet 2006;45:13–31.
22. Durand P, Debray D, Kolaci M, Bouligand J, Furlan V, Fabre M, et al. Tacrolimus dose requirement in pediatric liver transplantation: influence of CYP3A5 gene polymorphism. Pharmacogenomics 2013;14:1017–25.
23. Bedewy AM, El-Maghraby SM. Do SLCO1B3 (T334G) and CYP3A5*3 polymorphisms affect response in Egyptian chronic myeloid leukemia patients receiving imatinib therapy? Hematology 2013;18:211–6.
24. Hyland PL, Freedman ND, Hu N, Tang ZZ, Wang L, Wang C, et al. Genetic variants in sex hormone metabolic pathway genes and risk of esophageal squamous cell carcinoma. Carcinogenesis 2013;34:1062–8.
25. Picard N, Rouguieg-Malki K, Kamar N, Rostaing L, Marquet P. CYP3A5 genotype does not influence everolimus *in vitro* metabolism and clinical pharmacokinetics in renal transplant recipients. Transplantation 2011;91:652–6.
26. Dandara C, Ballo R, Parker MI. CYP3A5 genotypes and risk of esophageal cancer in two South African populations. Cancer Lett 2005;225:275–82.
27. Tsunedomi R, Iizuka N, Hamamoto Y, Uchimura S, Miyamoto T, Tamesa T, et al. Patterns of expression of cytochrome P450 genes in progression of hepatitis C virus-associated hepatocellular carcinoma. Int J Oncol 2005;27:661–7.
28. El Mouelhi M, Didolkar MS, Elias EG, Guengerich FP, Kauffman FC. Hepatic drug-metabolizing enzymes in primary and secondary tumors of human liver. Cancer Res 1987;47:460–6.

29. Philip PA, Kaklamanis L, Ryley N, Stratford I, Wolf R, Harris A, et al. Expression of xenobiotic-metabolizing enzymes by primary and secondary tumors in man. Int J Radiation Oncol Biol Phys 1994;29:277–83.
30. Sabatini DM. mTOR and cancer: insights into a complex relationship. Nat Rev Cancer 2006;6:729–34.
31. Wang Z, Zhong J, Inuzuka H, Gao D, Shaik S, Sarkar FH, et al. An evolving role for Deptor in tumor development and progression. Neoplasia 2012; 14:368–75.
32. Oh WJ, Jacinto E. mTOR complex 2 signaling and functions. Cell Cycle 2011;10:2305–16.
33. Razmara M, Heldin CH, Lennartsson J. Platelet-derived growth factor-induced Akt phosphorylation requires mTOR/Rictor and phospholipase C-γ1, whereas S6 phosphorylation depends on mTOR/Raptor and phospholipase D. Cell Commun Signal 2013;11:3–14.
34. Xu Y, Lai E, Liu J, Lin J, Yang C, Jia C, et al. IKK interacts with rictor and regulates mTORC2. Cell Signal 2013;25:2239–45.
35. Pignochino Y, Dell'Aglio C, Basiricò M, Capozzi F, Soster M, Marchiò S, et al. The combination of Sorafenib and Everolimus abrogates mTORC1 and mTORC2 upregulation in osteosarcoma preclinical models. Clin Cancer Res 2013;19:2117–31.
36. Sarbassov DD, Ali SM, Sengupta S, Sheen JH, Hsu PP, Bagley AF, et al. Prolonged rapamycin treatment inhibits mTORC2 assembly and Akt/PKB. Mol Cell 2006;22:159–68.
37. Joha S, Nugues AL, Hétuin D, Berthon C, Dezitter X, Dauphin V, et al. GILZ inhibits the mTORC2/AKT pathway in BCR-ABL (+) cells. Oncogene 2012;31:1419–30.
38. Sparks CA, Guertin DA. Targeting mTOR: prospects for mTOR complex 2 inhibitors in cancer therapy. Oncogene 2010;29:3733–44.
39. Dames SA, Mulet JM, Rathgeb-Szabo K, Hall MN, Grzesiek S. The structure of the FATC domain of the protein kinase target of rapamycin suggests a role for redox-dependent structural and cellular stability. J Biol Chem 2005;280:20558–64.
40. Neklesa TK, Davis RW. Superoxide anions regulate TORC1 and its ability to bind Fpr1: rapamycin complex. Proc Natl Acad Sci U S A 2008;105: 15166–71.
41. Tan CY, Hagen T. Post-translational regulation of mTOR complex 1 in hypoxia and reoxygenation. Cell Signal 2013;25:1235–44.
42. Kumari Kanchan R, Tripathi C, Singh Baghel K, Kumar Dwivedi S, Kumar B, Sanyal S, et al. Estrogen receptor potentiates mTORC2 signaling in breast cancer cells by up-regulating superoxide anions. Free Radic Biol Med 2012;53:1929–41.
43. Wang RH, Kim HS, Xiao C, Xu X, Gavrilova O, Deng CX. Hepatic Sirt1 deficiency in mice impairs mTORC2/Akt signaling and results in hyperglycemia, oxidative damage, and insulin resistance. J Clin Invest 2011;121: 4477–90.
44. Ethier C, Tardif M, Arul L, Poirier GG. PARP-1 modulation of mTOR signaling in response to a DNA alkylating agent. PLoS ONE 2012;7: e47978.
45. Martin KR, Barrett JC. Reactive oxygen species as double-edged swords in cellular processes: low-dose cell signaling versus high-dose toxicity. Hum Exp Toxicol 2002;21:71–5.
46. Wang J, Yi J. Cancer cell killing via ROS: to increase or decrease, that is the question. Cancer Biol Ther 2008;7:1875–84.
47. Gupta SC, Hevia D, Patchva S, Park B, Koh W, Aggarwal BB. Upsides and downsides of reactive oxygen species for cancer: the roles of reactive oxygen species in tumorigenesis, prevention, and therapy. Antioxid Redox Signal 2012;16:1295–322.
48. Li M, Zhao L, Liu J, Liu A, Jia C, Ma D, et al. Multi-mechanisms are involved in reactive oxygen species regulation of mTORC1 signaling. Cell Signal 2010;22:1469–76.

Published OnlineFirst February 3, 2015; DOI: 10.1158/0008-5472.CAN-14-1589

Cancer Research
The Journal of Cancer Research (1916–1930) | The American Journal of Cancer (1931–1940)

AACR American Association for Cancer Research

CYP3A5 Functions as a Tumor Suppressor in Hepatocellular Carcinoma by Regulating mTORC2/Akt Signaling

Feng Jiang, Lei Chen, Ying-Cheng Yang, et al.

Cancer Res 2015;75:1470-1481. Published OnlineFirst February 3, 2015.